Fitoterapia 137 (2019) 104252

Contents lists available at ScienceDirect

Fitoterapia

journal homepage: www.elsevier.com/locate/fitote

Phenolic compounds from the stems of *Fissistigma polyanthoides* and their anti-oxidant activities

Hieu Nguyen Ngoc[a], Lisa Mair[b], Duc Trong Nghiem[c], Kim Le Thien[c], Johanna M. Gostner[b], Hermann Stuppner[a], Markus Ganzera[a,*]

[a] Institute of Pharmacy, Pharmacognosy, Center for Molecular Biosciences (CMBI), University of Innsbruck, 6020 Innsbruck, Austria
[b] Division of Medical Biochemistry, Biocenter, Medical University of Innsbruck, 6020 Innsbruck, Austria
[c] Department of Botany, Hanoi University of Pharmacy, 13-15 Le Thanh Tong, Hoan Kiem, Hanoi 100000, Viet Nam

ARTICLE INFO

Keywords:
Fissistigma polyanthoides
Phenolic
Flavonoid
Anti-oxidant

ABSTRACT

The stems of *Fissistigma polyanthoides* (A.DC.) Merr. are traditionally used for the treatment of rheumatism and for recuperating women after childbirth. In our continuous phytochemical investigation of this plant, four new (**1**, **2**, **5**, and **19**) and fifteen known (**3**, **4**, and **6–18**) phenolic compounds were isolated. The structures of all compounds were elucidated based on extensive spectroscopic analyses (1D-, 2D-NMR, and MS), and in comparison with reported literature data. The new natural products showed to be two poly-methoxylated chalcones (**1** and **2**) and two flavonoid glycosides, with **19** containing an uncommon sugar moiety (quinovose). Compounds with sufficient amount were tested for their anti-oxidant activity in a cell-based assay using the human bronchial epithelial cell line BEAS-2B. The compounds' capacity to inhibit the peroxyl radical triggered formation of dichlorofluorescein (DCF) was investigated in a dose-dependent manner. Both, anti-oxidant (**3**, **4**, **6**, **8–12**, and **14**) and pro-oxidative (**5** and **16**) properties were found for the investigated substances. The half maximal concentrations (IC_{50}) for the inhibition of ROS formation ranged between 18.8 µM and 63.5 µM. Compounds, which acted protectively in the cellular antioxidant activity (CAA) assay and did not negatively affect cell viability, could be interesting targets for further investigations.

1. Introduction

Fissistigma polyanthoides (A.DC.) Merr., an up-to 10 m tall climber of the Annonaceae family, is widely distributed in South Eastern Asia (southern China, Myanmar, Thailand and Vietnam). The plant has oblong-lanceolate, leathery leaves with a length of up to 20 cm, reddish flowers arranged in a pseudo-cymose, and oblong, brown seeds [1]. In northern Vietnam, the stems are an ingredient of herbal bath therapy for women after childbirth, whereas in China they are traditionally used for the treatment of inflammation and rheumatism. However, the plant has not been investigated phytochemically, with the exception of one paper describing three flavonoids (methoxylated flavone, flavanone, and one chalcone) and one alkaloid (thaipetaline) as chemical constituents of the bark [2]. The present work was performed to study the phenolic profile in the stems comprehensively, and to investigate the relevance of these constituents for the traditional use of *F. polyanthoides*.

A number of plant constituents, which are of interest for further phytopharmaceutical use share one common property, which is the ability to inhibit or prevent oxidation processes. Such antioxidant substances should protect cells against the damaging effects of free radical overproduction or oxidative stress, whereby the detailed biochemical mechanisms may differ [3]. Phenolic compounds are known for their radical scavenging properties, metal ion chelation, and enzymatic inhibition during the production of reactive oxygen species (ROS). The latter are associated with oxidative stress and protein oxidation. Additionally, an overproduction of ROS also causes tissue injury, another initiator of inflammatory processes [4]. Therefore, we investigated the ability of the isolated compounds to interfere with ROS production in human lung epithelial cells, which could explain the traditional use of *F. polyanthoides* as anti-inflammatory drug.

2. Experimental

2.1. General experimental procedures

NMR experiments were performed on an Avance II 600 spectrometer (Bruker) at 600.19 MHz (^{1}H) and 150.91 MHz (^{13}C). The samples

* Corresponding author at: Institute of Pharmacy, Pharmacognosy, University of Innsbruck, Innrain 80-82, 6020 Innsbruck, Austria.
E-mail address: markus.ganzera@uibk.ac.at (M. Ganzera).

https://doi.org/10.1016/j.fitote.2019.104252
Received 15 May 2019; Received in revised form 24 June 2019; Accepted 1 July 2019
Available online 02 July 2019

were prepared in suitable deuterated solvents from Eurisotop using tetramethylsilane (TMS) as reference. For LC-MS studies, an Esquire 3000 ion trap mass spectrometer (Bruker) equipped with ESI source was coupled to an Agilent 1100 series HPLC instrument. HRESIMS spectra were recorded on a micrOTOF-Q II MS (Bruker) operated by Hystar software. Optical rotation was measured on a Perkin Elmer Polarimeter 341 with 10.0 cm tube, IR spectra on an Alpha FT-IR spectrometer (Bruker), and circular dichroism (CD) spectra on a J-715 spectropolarimeter (Jasco). Chromatographical techniques employed for the isolation of individual constituents included flash chromatography on a Reveleris® (Büchi) system and open columns, filled with silica-gel and reversed-phase material (RP-C18), as well as Sephadex LH-20 (Sigma-Aldrich). Final purifications were achieved on a semi-preparative Dionex HPLC system with a P580 pump, ASI 100 automated sample injector, UVD 170 U detector, and Gilson Ambimed 206 fraction collector; the stationary phase used was a Synergi MAX-RP 80A column (250 × 10 mm, 4 µm) from Phenomenex.

2.2. Plant material and chemicals

Fissistigma polyanthoides stems were collected in Sa Pa, Lao Cai, Vietnam in November 2016. The sample was botanically authenticated by MSc. Duc Trong Nghiem from the Department of Botany, Hanoi University of Pharmacy, Hanoi, Viet Nam. A voucher specimen (2016/11-FPa) is deposited at the Institute of Pharmacy, Pharmacognosy, University of Innsbruck, Innsbruck, Austria.

All solvents required for extraction and isolation were purchased from VWR international. Ultrapure water was produced by an Arium 611 UV (Sartorius) system.

2.3. Extraction and isolation

The dried stems of *Fissistigma polyanthoides* (2.1 kg) were extracted with MeOH in an ultrasonic bath (5 L × 1 h × 5 times, Bandelin Sonorex 35 KHz) at ambient temperature. The extracts were combined and then evaporated *in vacuo* to yield a green slurry (152.3 g). The extract was suspended in distilled water and partitioned with EtOAc and *n*-BuOH.

The EtOAc soluble portion (45.5 g) was fractionated on an open normal-phase (NP) silica gel column (40–63 µm particle size) using a solvent gradient consisting of petroleum ether and acetone (from 20:1 to 0:1), to yield 16 fractions (FPE 1–16). Fraction FPE 7 (0.6 g) was subjected to flash-chromatography using a RP-C18 cartridge and gradient elution (50–85% MeOH in water), resulting in the isolation of compounds **2** (1.5 mg) and **13** (0.9 mg). The same approach was applied to fraction FPE 10 (1.2 g), leading to the purification of compounds **1** (32.6 mg) and **15** (7.1 mg). Fraction FPE 15 (3.5 g) was fractionated on an RP-C18 column (MeOH gradient from 30 to 90%) to obtain six subfractions (FPE 15.1–6). From the concentrated methanol solution of FPE 15.6 (0.8 g) fine yellowish crystals precipitated, which were removed by centrifugation and washed with cold MeOH to obtain compound **5** (17.2 mg). The largest fraction FPE 16 (8.4 g) was separated in 11 subfractions (FPE 16.1–11) also using a RP-C18 column (MeOH gradient from 30 to 90%). Fraction FPE 16.3 (1.0 g) was then subjected to size-exclusion chromatography (Sephadex LH-20, MeOH as mobile phase) to yield compound **9** (50.2 mg). The same strategy was selected to purify compounds **3** (30.1 mg), **4** (51.3 mg), **6** (10.8 mg), and **14** (35.8 mg) from FPE 16.5 (1.5 g), as well as compound **16** (4.6 mg) from FPE 16.8 (1.5 g). FPE 16.7 (0.8 g) was also fractionated on a Sephadex LH-20 column first, followed by semi-preparative HPLC. Under isocratic conditions (40% MeCN in 0.1% formic acid) compounds **17** (4.2 mg, t_R = 24.5 min) and **18** (3.4 mg, t_R = 18.4 min) could be obtained.

The *n*-BuOH soluble portion (62.4 g) was initially fractionated on a silica gel column with the solvent system EtOAc/MeOH (from 20:1 to 0:1), resulting in 8 fractions (FPB 1–8). Fraction FPB 3 (0.8 g) was subjected to RP-C18 column chromatography (gradient 30–90% MeOH) and finally purified on Sephadex LH-20 material, eluting with MeOH, to obtain compound **19** (1.9 mg). Fraction FPB 5 (2.0 g) was first fractionated on a RP-C18 column with gradient elution (10–80% MeOH) to receive 90 mg of FPB 5.4, which contained three major peaks. By semi-preparative HPLC (0–30 min: isocratic 13% MeCN in water) compounds **10** (9.0 mg, t_R = 20.7 min), **12** (7.6 mg, t_R = 26.9 min), and **11** (10.5 mg, t_R = 29.5 min) were isolated. Fraction FPB 8 (1.5 g) was fractionated on a RP column (5–80% MeOH) and finally purified by semi-preparative HPLC (0–45 min: isocratic 19% MeCN in water) to yield compounds **7** (5.4 mg, t_R = 34.7 min) and **8** (5.6 mg, t_R = 40.2 min).

Table 1
^{1}H and ^{13}C NMR spectroscopic data for compounds **1** and **2** (δ in ppm, J in Hz).

Pos.	**1**[a]				**2**[a]			
	δ_C	*mult.*	δ_H	*mult., J*	δ_C	*mult.*	δ_H	*mult., J*
1	111.6	s			116.3[d]	s		
2	146.0	s			143.5	s		
3	136.1	s			136.7	s		
4[b]	140.0	s			139.8	s		
5[b]	148.4	s			145.1	s		
6	150.3	s			148.1[d]	s		
7	135.7	d	8.08	d, 16.2	18.7	t	3.02	t, 7.2
8	124.8	d	8.11	d, 16.2	38.9	t	3.28	t, 7.2
9	191.8	s			200.9	s		
1´	138.9	s			136.7	s		
2´	128.7	d	8.03	d, 7.5	128.3	d	8.00	d, 7.8
3´	128.6	d	7.48	t, 7.5	128.5	d	7.45	t, 7.8
4´	132.5	d	7.55	t, 7.5	133.1	d	7.55	t, 7.8
5´	128.6	d	7.48	t, 7.5	128.5	d	7.45	t, 7.8
6´	128.7	d	8.03	d, 7.5	128.3	d	8.00	d, 7.8
3-OMe	61.6	q	3.93	s	61.3	q	3.91	s
4-OMe[c]	61.3	q	4.00	s	61.3	q	3.84	s
5-OMe[c]	61.7	q	3.86	s	61.2	q	3.93	s
6-OMe	61.5	q	3.89	s	61.3	q	3.85	s
2-OH			6.53	s			6.37	s

[a] in $CDCl_3$ (600 MHz for ^{1}H, 150 MHz for ^{13}C); [b,c] interchangeable signals.
[d] The chemical shifts were assigned based on HMBC crosspeaks due to low carbon signal intensity (± 0.3 ppm).

2.3.1. (E)-2-hydroxy-3,4,5,6-tetramethoxychalcone (1)

Brownish oil; IR ν_{max} 3369, 1740, 1446, 1376, 1043 cm^{-1}; UV λ_{max} 228, 262, 340 nm; See Table 1 for ^{1}H NMR (600 MHz) and ^{13}C NMR (150 MHz) spectroscopic data; HRESIMS *m/z* 367.1147 $[M + Na]^+$ (calcd. for $C_{19}H_{20}O_6Na$ 367.1152).

2.3.2. 2-Hydroxy-3,4,5,6-tetramethoxydihydrochalcone (2)

Colorless oil; IR ν_{max} 3409, 2937, 1713, 1466, 1416, 1037 cm^{-1}; UV λ_{max} 241, 285 nm; See Table 1 for ^{1}H NMR (600 MHz) and ^{13}C NMR (150 MHz) spectroscopic data; HRESIMS *m/z* 369.1308 $[M + Na]^+$ (calcd. for $C_{19}H_{22}O_6Na$ 369.1309).

2.3.3. Quercetin 3-methoxy-3′-O-α-L-rhamnopyranosyl-(1 → 2)-β-D-glucopyranoside (5)

Yellowish gum; $[\alpha]_D^{20}$ -30.0 (*c* 0.08, MeOH); IR ν_{max} 3306, 1651, 1354, 1014 cm^{-1}; UV λ_{max} 251, 267, 355 nm; See Table 2 for ^{1}H NMR (600 MHz) and ^{13}C NMR (150 MHz) spectroscopic data; HRESIMS *m/z* 647.1568 $[M + Na]^+$ (calcd. for $C_{28}H_{32}O_{16}Na$ 647.1583).

2.3.4. (2R, 3R)-taxifolin 3-O-β-D-quinovopyranoside (19)

Yellowish gum; $[\alpha]_D^{20}$ -7.5 (*c* 0.07, MeOH); IR ν_{max} 3272, 1634, 1259, 1165, 1064 cm^{-1}; UV λ_{max} 292 nm; CD (MeOH, mdeg) $[\theta]_{298}$–3.1, $[\theta]_{326}$ + 1.2; See Table 2 for ^{1}H NMR (600 MHz) and ^{13}C NMR (150 MHz) spectroscopic data; HRESIMS *m/z* 473.1049 $[M + Na]^+$ (calcd. for $C_{21}H_{22}O_{11}Na$ 473.1054).

Table 2
^{1}H and ^{13}C NMR spectroscopic data for compounds **5** and **19** (δ in ppm, J in Hz).

Pos.	**5**[a]				**19**[b]			
	δ_C	*mult.*	δ_H	*mult., J*	δ_C	*mult.*	δ_H	*mult., J*
2	155.3	s			83.5	d	5.28	d, 8.4
3	137.7	s			77.5	d	4.72	d, 8.4
4	177.9	s			195.6	s		
5	161.2	s			165.5	s		
6	98.6	d	6.20	d, 1.8	97.3	d	5.90	s
7	164.1	s			169.1	s		
8	93.9	d	6.49	d, 1.8	96.3	d	5.90	s
9	156.4	s			164.0	s		
10	104.2	s			102.6	s		
1′	120.6	s			129.0	s		
2′	116.1	d	7.74	d, 1.8	115.6	d	6.91	d, 1.8
3′	144.8	s			146.5	s		
4′	150.4	s			147.2	s		
5′	116.1	d	7.00	d, 8.4	116.1	d	6.76	d, 7.8
6′	123.4	d	7.64	dd, 1.8, 8.4	120.7	d	6.78	dd, 7.8, 1.8
	Glucose				Quinovose			
1″	98.7	d	5.12	d, 7.2	102.4	d	3.99	d, 7.8
2″	76.9	d	3.58	dd, 7.2, 9.0	74.8	d	3.21	dd, 7.8, 9.0
3″	77.3	d	3.49	m	77.4	d	3.12	t, 9.0
4″	69.6	d	3.25	m	76.8	d	2.94	t, 9.0
5″	76.9	d	3.34	m	73.6	d	3.02	m
6″	60.4	t	3.51	m	17.9	q	1.17	d, 6.0
			3.68	dd, 4.8, 11.4				
	Rhamnose							
1‴	100.5	d	5.19	brs				
2‴	70.5	d	3.73	m				
3‴	70.5	d	3.43	m				
4‴	72.0	d	3.18	m				
5‴	68.5	d	3.86	m				
6‴	18.0	q	1.09	d, 6.0				
OMe	59.7	q	3.80	s				

[a] in DMSO-d_6; [b] in MeOH-d_4 (600 MHz for ^{1}H, 150 MHz for ^{13}C).

2.4. Acid hydrolysis of 5 and GC–MS analysis of sugars

Compound **5** (3.0 mg) was stirred with 1 mL 1 N HCl in MeOH for 3 h at 60 °C in a sand bath. The reaction mixture was neutralized and partitioned with EtOAc (3 times × 1 mL), the water layers were combined and dried to obtain 2.0 mg of sugar fraction for analysis.

The sugar fraction was derivatized with L-cysteine methyl ester hydrochloride (1.5 mg in 200 µL pyridine, 60 °C, 1 h), subsequently silylated with BSTFA and TMCS (99:1, *v*/v; 200 µL, 60 °C, 1 h) and analysed by GC–MS. Reference compounds D-glucose (t_R = 78.71 min) and L-rhamnose (t_R = 75.93 min) were derivatized and analysed using the same protocol. D-glucose (t_R = 78.69 min) and L-rhamnose (t_R = 75.86 min) were detected in **5**. The GC–MS analyses were performed on an Agilent 5975C Series GC/MSD system equipped with an Agilent 7693 autosampler, Triple AxisDetector (MS), and Agilent 7890A GC System with an Agilent HP-5MS (30 m × 250 µm × 0.25 µm) column. The GC–MS condition were set up as follows: starting at 70 °C for 2 min, then 2 °C/min to 150 °C (hold 150 °C for 2 min), then 5 °C/min to 220 °C (hold 220 °C for 15 min), then 15 °C/min to 300 °C (hold 300 °C for 10 min), total run time 88.33 min; injection volume 1 µL; split ratio 10:1; carrier gas helium; flow rate 7.5 mL/min.

2.5. Cellular antioxidant activity assay

The human bronchial epithelial cell line BEAS-2B (ATCC) was cultured in Roswell Park Memorial Institute's medium (RPMI; Sigma-Aldrich) supplemented with 10% fetal bovine serum (FBS; Life Technologies) under standard conditions at 37 °C and 5% (*v*/v) CO_2.

The intracellular antioxidant activity was determined based on the original protocol from Wolfe and Liu [5] using 2′,7′-dichlorofluorescein diacetate (DCFH-DA) as a substrate. DCFH-DA passes the cell membrane where it is trapped after being deacetylated by intracellular esterases. DCFH can be oxidized to the fluorescent 2′,7′-dichlorofluorescein (DCF) by reactive oxygen species (ROS).

For testing, a cell suspension containing 2×10^4 cells/ 100 µL/ well was seeded in a 96-well plate and incubated for 24 h . Cells were washed twice with prewarmed phosphate buffered saline (PBS; Sigma-Aldrich). Then each well was treated with 50 µL of 25 µM DCFH-DA (Sigma-Aldrich) dissolved in Hanks' balanced salt solution (HBSS; Sigma-Aldrich). After incubation for 1 h, cells were treated with the 14 test compounds at concentrations ranging from 3.1 µM to 25 µM. As a positive control, 10 µM quercetin (Sigma-Aldrich) was applied, and 0.05% dimethyl sulfoxide (DMSO) in HBSS (*v*/v) was used as solvent control. Again, the cells were incubated for 1 h. Then cells were washed with PBS and treated with 600 µM of the peroxyl radical generator 2,2′-azobis(2-methylpropionamidine) dihydrochloride (AAPH; Sigma-Aldrich) dissolved in HBSS. The cells were incubated for 30 min protected from light. The fluorescence of DCF (excitation 485 nm/ emission 535 nm) was measured on a Tecan infinite F200 PRO plate reader. The intensity of the fluorescence signal reflects the level of intracellular ROS.

To investigate cell viability and cytotoxic effects, the resazurin-based fluorescence assay CellTiter-Blue (CTB; Promega) was applied. After treating the cells with the test compounds and incubating for 24 h, 10% (*v*/v) of the CTB reagent were added to the medium. After 1 h of incubation the conversion of resazurin to resorufin was measured on a Tecan infinite F200 Pro plate reader (560 nm excitation/ 590 nm emission). Half maximal inhibitory concentrations (IC_{50}) were calculated by using the CalcuSyn software (Biosoft) [6].

3. Results and discussion

Four new (**1**, **2**, **5**, and **19**), along with fifteen known (**3**, **4**, and **6–18**) compounds were isolated from *F. polyanthoides* stems, their chemical structures (Fig. 1) were elucidated through a combination of 1D-, 2D-NMR, and HR-ESI-MS experiments.

Compound **1** was isolated as brownish oil. Its molecular formula was established as $C_{19}H_{20}O_6$ by a $[M + Na]^+$ peak at *m/z* 367.1147 (calcd for $C_{19}H_{20}O_6Na$ 367.1152) in the HR-ESI-MS spectrum. The IR spectrum showed absorption bands at 3369 and 1740 cm^{-1}, which corresponded to hydroxyl and carbonyl functionalities, respectively. The ^{13}C NMR displayed 14 carbons in the range of 100–150 ppm, which indicated two benzene rings and one double bond in the structure, along with one ketone group at δ_C 191.8, suggesting a chalcone-type flavonoid. The ^{1}H NMR data showed the characteristic pattern of a phenyl moiety with the co-appearance of three signals at δ_H 8.03 (2H, d, J = 7.5 Hz), 7.48 (2H, t, J = 7.5 Hz), and 7.55 (1H, t, J = 7.5 Hz), while a *trans*-type double bond was determined by the large coupling constant of two protons at δ_H 8.08 (1H, d, J = 16.2 Hz) and 8.11 (1H, d, J = 16.2 Hz) (Table 1). Moreover, four methoxyl groups at δ_H 4.00 (3H, s), 3.93 (3H, s), 3.89 (3H, s), and 3.86 (3H, s) were determined to link with carbons (δ_C 140.0, 136.1, 150.3, and 148.4, respectively) of the second benzene ring. The substitution pattern was assigned based on HMBC correlations from 2-OH (δ_H 6.53) to C-1/2/3 (δ_C 111.6, 146.0, and 136.1), as well as from H-7 (δ_H 8.08) to C-1/2/6 (δ_C 111.6, 146.0, and 150.3) (Fig. 2). Therefore, the structure of **1** was established as (*E*)-2-hydroxy-3,4,5,6-tetramethoxychalcone, which was isolated for the first time from nature.

Compound **2** was obtained as colorless oil, its molecular formula showed to be $C_{19}H_{22}O_6$ based on a sodium adduct peak $[M + Na]^+$ at *m/z* 369.1308 (calcd for $C_{19}H_{22}O_6Na$ 369.1309). The IR spectrum revealed hydroxyl (3409 cm^{-1}) and carbonyl (1713 cm^{-1}) bands. The ^{1}H and ^{13}C NMR spectra of **2** were similar to those of **1**, except for the appearance of two triplet-shaped proton signals at δ_H 3.02 (2H, t, J = 7.2 Hz) and 3.28 (2H, t, J = 7.2 Hz), and two carbon signals at δ_C 18.7 and 38.9, indicating hydrogenation of the double bond (Table 1).

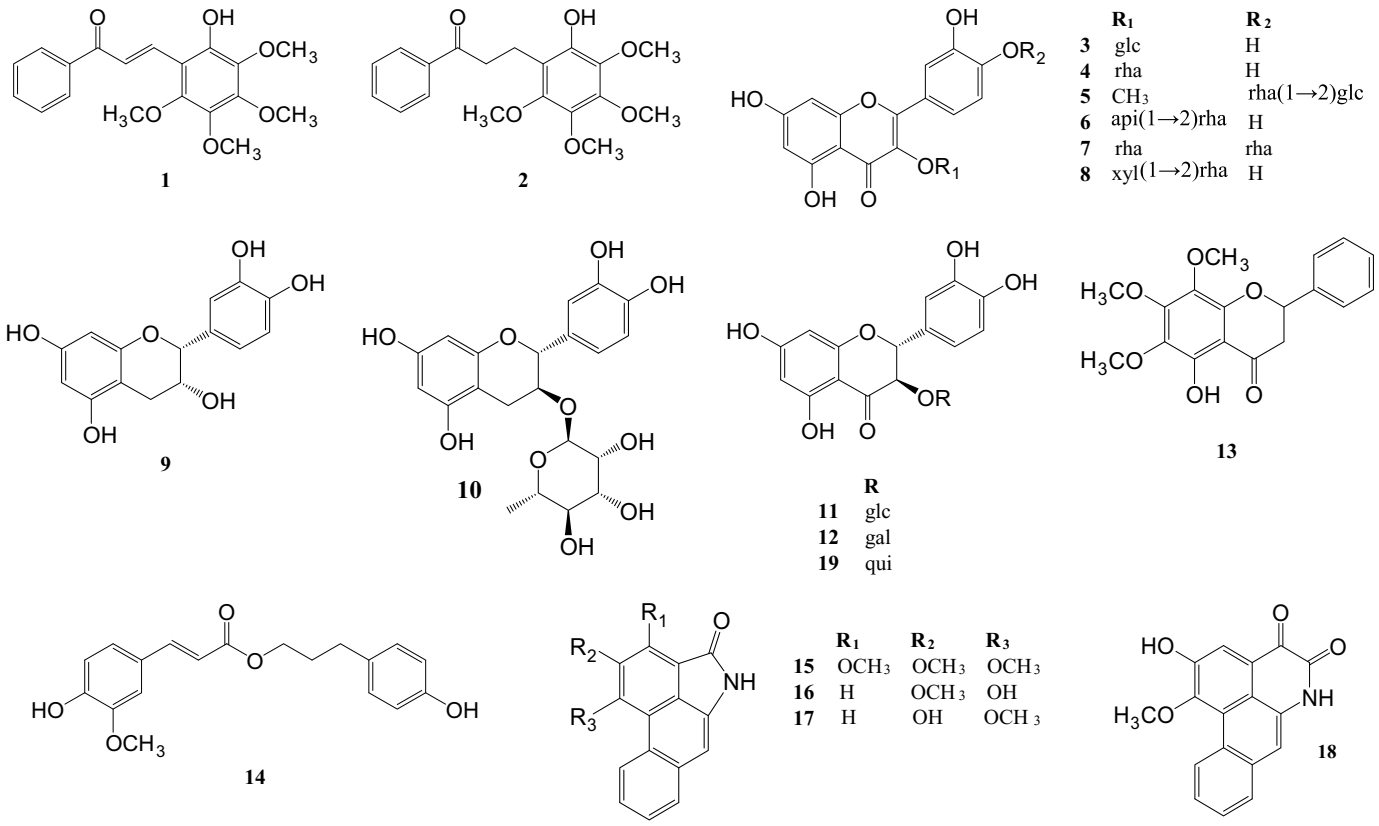

Fig. 1. Structures of isolated compounds from *Fissistigma polyanthoides* stems.

The key HMBC correlations from H-7 (δ_H 3.02) and H-8 (δ_H 3.28) to C-1 (δ_C 116.3) and C-9 (δ_C 200.9) also supported this deduction (Fig. 2). Collectively, the structure of **2** was determined as 2-hydroxy-3,4,5,6-tetramethoxydihydrochalcone, again a new natural product.

Because of an $[M + Na]^+$ ion at *m/z* 647.1568 (calcd for $C_{28}H_{32}O_{16}Na$ 647.1583), compound **5** was assigned the molecular formula $C_{28}H_{32}O_{16}$, corresponding to 13 double-bond equivalent indices. The IR spectrum showed characteristic bands for carbonyl (1651) and

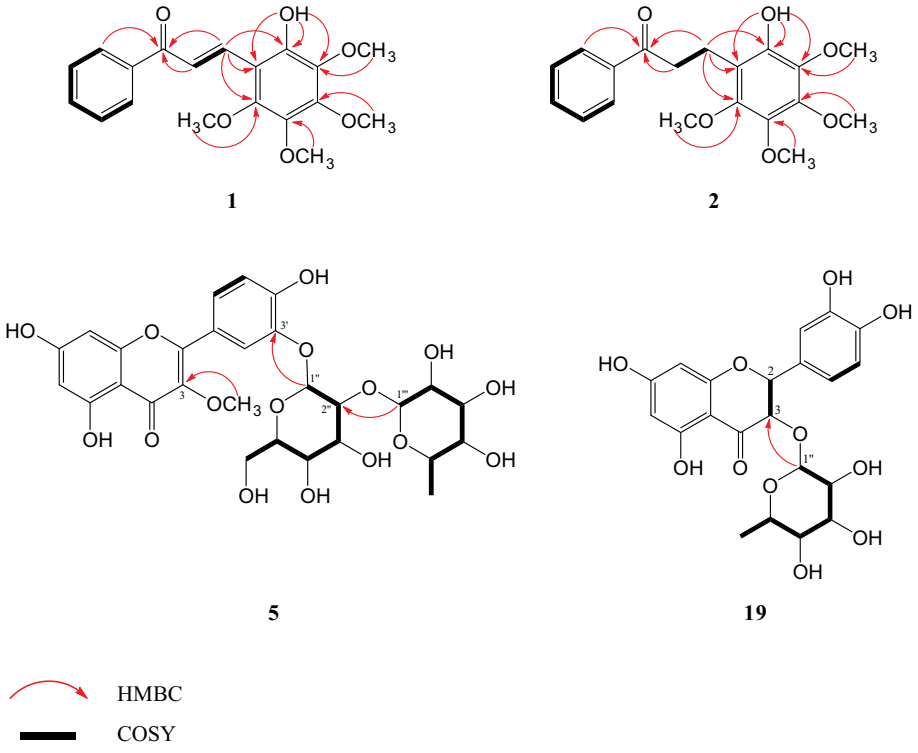

Fig. 2. Key HMBC (H → C) and $^1H-^1H$ COSY correlations of compounds **1**, **2**, **5** and **19**.

Table 3
Half maximal inhibitory concentration (IC_{50}) of compounds regarding the prevention of intracellular ROS formation in AAPH treated BEAS-2B cells.

Compounds	IC_{50} (μM)	(lower CI	–	upper CI)	R^2
1	59.9	15.1	–	237.4	0.9009
3	24.1	19.2	–	30.3	0.9916
4	18.8	18.0	–	19.7	0.9995
5	–	–		–	–
6	38.5	25.2	–	48.9	0.9835
7	–	–		–	–
8	35.3	14.0	–	89.5	0.9212
9	47.0	29.7	–	74.3	0.9842
10	47.9	28.7	–	79.8	0.9809
11	61.4	32.1	–	117.5	0.9758
12	63.5	38.3	–	105.4	0.9854
14	31.2	11.9		82.1	0.9044
15	–	–		–	–
16	–	–		–	–

hydroxyl (3306 cm^{-1}) functionalities, while the ^1H and ^{13}C NMR spectra indicated a quercetin backbone. Specifically, an ABX spin system at δ_H 7.74 (1H, d, J = 1.8 Hz), 7.64 (1H, dd, J = 1.8, 8.4 Hz), and 7.00 (1H, d, J = 1.8 Hz), two diagnostic aromatic protons of the A ring at δ_H 6.20 (1H, d, J = 1.8 Hz) and 6.49 (1H, d, J = 1.8 Hz), as well as a conjugated ketone at δ_C 177.9 (s). A methoxylation at position C-3 was deduced by a HMBC correlation from OMe (δ_H 3.80) to C-3 (δ_C 137.7). As for the glycone part, two sugar moieties were observed by the co-appearance of anomeric protons at δ_H 5.12 (1H, d, J = 7.2 Hz) and 5.19 (1H, brs) (Table 2). The COSY spectrum showed two coupling networks (Fig. 2) typical for two hexopyranose-type sugars, with one belonging to the deoxy type. The two sugars were determined to be *β*-D-glucopyranose and *α*-L-rhamnopyranose by analysis of NOESY data (Fig.S3.6, Supporting Information), by comparison with the ^{13}C NMR data of quercetin 3,7-dimethylether-3′-*O*-*α*-L-rhamnopyranosyl-(1 → 2)-*β*-D-glucopyranoside [7], as well as confirmed by GC–MS analysis of the hydrolysis product, compared with authentic sugars (L-rhamnose and D-glucose) (Fig.S3.8, Supporting Information). Linkage between the two sugars was confirmed by HMBC correlations from H-1‴ (δ_H 5.19) to C-2″ (δ_C 76.9) and from H-2″ (δ_H 3.58) to C-1‴ (δ_C 100.5), whereas the position of the glycone moiety became obvious by an HMBC crosspeak between H-1″ (δ_H 5.12) and C-3″ (δ_C 144.8) (Fig. 2). Thus, the structure of **5** could be assigned as quercetin 3-methoxy-3′–*O*-*α*-L-rhamnopyranosyl-(1 → 2)-*β*-D-glucopyranoside.

Compound **19** was also isolated as a yellow gum, and its molecular formula $C_{21}H_{22}O_{11}$ established by an ion peak at *m/z* 473.1049 ($[M + Na]^+$, calcd for $C_{21}H_{22}O_{11}Na$ 473.1054). The IR spectrum showed characteristic absorption bands for carbonyl (1634 cm^{-1}) and hydroxyl (3272 cm^{-1}) groups, respectively. The ^1H and ^{13}C NMR spectrum indicated the presence of an ABX spin system [δ_H 6.76 (d, J = 7.8 Hz), 6.78 (dd, J = 7.8, 1.8 Hz), and 6.91 (d, J = 1.8 Hz)], two *meta*-aromatic protons [δ_H 5.90 (s) and 5.90 (s)], two doublet signals [δ_H 4.72 (d, J = 8.4 Hz) and 5.28 (d, J = 8.4 Hz)], and a ketone resonance at δ_C 195.6, which are diagnostic signals for a flavanone skeleton (Table 2). Besides that, the proton resonances at δ_H 3.99 (1H, d, J = 7.8 Hz) and 1.17 (3H, d, J = 6.0 Hz) were typical for a deoxy-type sugar. The latter was determined as *β*-D-quinovopyranose by the large coupling constant (J = 7.8 Hz), NOESY correlations of H-3‴/ H-1‴, H-5‴ and H-4‴/ H-2″, H-6‴ (Fig.S4.6, Supporting Information), and in comparison with literature data [8]. A confirmation by hydrolysis/GC–MS as described before was not possible due to the limited amount of compound available. The binding position of *β*-D-quinovopyranose to the flavanone aglycon was established by an HMBC correlation of H-1″ (δ_H 3.99) to C-3 (δ_C 77.5) (Fig. 2). The large coupling constants of H-2 [δ_H 5.28 (d, J = 8.4 Hz)] and H-3 [δ_H 4.72 (d, J = 8.4 Hz)] indicated *trans* relationship [9], and the CD spectrum of **19** was identical to that of (2*R*, 3*R*)-taxifolin, so that the (2*R*, 3*R*) configuration of C-2 and C-3 (Fig.S4.7, Supporting Information) can be assumed [9]. Therefore, the structure of **19** was elucidated as (2*R*, 3*R*)-taxifolin 3-*O*-*β*-D-quinovopyranoside.

Additionally, fifteen known compounds (**3**, **4**, and **6–18**) were isolated and identified as follows: quercetin 3-*O*-*β*-D-glucopyranoside (**3**) [10], quercetin 3-*O*-*α*-L-rhamnopyranoside (**4**) [11], quercetin 3-*O*-*β*-D-apiofuranosyl-(1 → 2)-*α*-L-rhamnopyranoside (**6**) [12], quercetin 3,3′-*O*-di-*α*-L-rhamnopyranoside (**7**) [13], quercetin 3-*O*-*β*-D-xylopyranosyl-(1 → 2)-α-L-rhamnopyranoside (**8**) [14], epicatechin (**9**) [15], catechin 3-*O*-*α*-L-rhamnopyranoside (**10**) [16], (2*R*,3*R*)-taxifolin 3-*O*-*β*-D-glucopyranoside (**11**) [17], (2*R*,3*R*)-taxifolin 3-*O*-*β*-D-galactopyranoside (**12**) [17,18], 5-hydroxy-6,7,8-trimethoxyflavanone (**13**) [19], *p*-hydroxyphenethyl-*trans*-ferulate (**14**) [20], piperolactam C (**15**) [21], piperolactam A (**16**) [22], aristololactam AII (**17**) [23], and 4,5-dioxodehydroasimilobine (**18**) [24]. NMR and MS data of the known compounds are provided as supplementary information in Tables S1 to S6.

Compounds that were available in sufficient amount (≥ 5.0 mg) were tested for their antioxidant capacity against the human bronchial epithelial cells BEAS-2B. They were treated with the peroxyl radical generator AAPH to increase ROS levels. The well-known antioxidant quercetin was able to reduce the intracellular ROS formation by approximately 60% at a concentration of 10 μM. For some compounds, *e.g.* compounds **3**, **4**, **6**, **8–12**, and **14**, a significant and dose-dependent inhibition of ROS formation was found, whereby compounds **3** and **4** were most active, with half maximal inhibitory concentrations (IC_{50}) of 24.1 and 18.8 μM. However, some substances showed pro-oxidative properties, for example compounds **5** and **16**. The antioxidant activities of all tested compounds are summarized in Fig.S5 (Supporting Information), and the IC_{50} values including lower and upper confidence intervals are given in Table 3. When studying a possible structure-activity-relationship of the investigated flavonoids the following trends were noticed: ROS inhibition correlated with the number of OH groups (see **4** and **7**), flavones were more active than flavanones (**3** and **11**), and the substitution of C3 with a disaccharide instead of a monosaccharide slightly reduced activity (**4** and **6**); all these observations were according to literature [25]. More unexpected were similar results for the two catechin derivatives **9** and **10**, because a free OH group in position C3 is usually associated with a stronger antioxidant capacity; a different stereochemical arrangement at this position could be a possible explanation [25]. Cell viability was strongly affected by compound **1** (IC_{50} = 36.1 μM), and somewhat by compounds **15** (IC_{50} = 394.5 μM) and **16** (IC_{50} = 179.2 μM), while the other compounds did not show any cytotoxicity within the tested concentration range (3.1 μM to 25 μM).

4. Conclusions

The continuous phytochemical investigation of *Fissistigma polyanthoides* stems resulted in the isolation and characterization of four new natural products (**1**, **2**, **5**, and **19**), along with fifteen known (**3**, **4**, and **6–18**), yet for *F. polyanthoides* new constituents. Concerning the latter, it is noteworthy to say that lactams like **15–17** are typical for species from the Annonaceae family and that these compounds are nephrotoxic [26]. Compounds **1** and **2** represent new polymethoxylated chalcones, while compounds **5** and **19** are previously undescribed flavone glycosides, partly substituted with rare sugar moieties. When evaluating the potential anti-oxidant activity of fourteen of the isolated compounds, substances **3** and **4** turned out to be interesting candidates for further investigations, because of their non-toxic nature and pronounced ability of inhibiting ROS formation in a dose-dependent manner. They therefore might explain, or at least significantly contribute to, the activity of *F. polyanthoides* stems if used as an anti-inflammatory remedy.

Declaration of Competing Interest

The authors declare no conflict of interest.

Acknowledgments

This study was conducted within the project “China-TCM cluster” and financially supported by the Austrian Federal Ministry of Health and the Austrian Federal Ministry of Science, Research and Economy (BMWFW-402.000/0016-WF/V/6/2016).

Appendix A. Supplementary data

NMR and HRESIMS data of isolated compounds (**1–19**), as well as their antioxidant capacity in the human bronchial epithelial cells BEAS-2B bioassay can be found online as supplementary data at https://doi.org/10.1016/j.fitote.2019.104252.

References

[1] Flora of China, Vol. 19, pp. 705–708.
[2] V. Jongbunprasert, R. Bavovada, P. Theraratchailert, R. Rungserichai, K. Likhitwitayawuid, Chemical constituents of *Fissistigma polyanthoides*, ScienceAsia 25 (1999) 31–33.
[3] V.A. Kostyuk, A.I. Potapovich, Mechanisms of the suppression of free radical overproduction by antioxidants, Front. Biosci. (Elite Ed.) 1 (2009) 179–188.
[4] N. Yahfoufi, N. Alsadi, M. Jambi, C. Matar, The immunomodulatory and anti-inflammatory role of polyphenols, Nutrients 10 (2018) 1618.
[5] K.L. Wolfe, R.H. Liu, Cellular antioxidant activity (CAA) assay for assessing antioxidants, foods, and dietary supplements, J. Agric. Food Chem. 55 (2007) 8896–8907.
[6] T.C. Chou, P. Talalay, Quantitative analysis of dose-effect relationships: the combined effects of multiple drugs or enzyme inhibitors, Adv. Enzym. Regul. 22 (1984) 27–55.
[7] A. Sinz, R. Matusch, T. Santisuk, S. Chaichana, V. Reutrakul, Flavonol glycosides from *Dasymaschalon sootepense*, Phytochemistry 47 (1998) 1393–1396.
[8] H.J. Zhang, E. Rumschlag-Booms, Y.F. Guan, D.Y. Wang, K.L. Liu, W.F. Li, V.H. Nguyen, N.M. Cuong, D.D. Soejarto, H.H.S. Fong, L. Rong, Potent inhibitor of drug-resistant HIV-1 strains identified from the medicinal plant *Justicia gendarussa*, J. Nat. Prod. 80 (2017) 1798–1807.
[9] A. Sakushima, K. Ohno, M. Coskun, K. Seki, K. Ohkura, Separation and identification of taxifolin 3-*O*-glucoside isomers from *Chamaecyparis obtusa* (Cupressaceae), Nat. Prod. Lett. 16 (2002) 383–387.
[10] Y. Zhang, D. Wang, L. Yang, D. Zhou, J. Zhang, Purification and characterization of flavonoids from the leaves of *Zanthoxylum bungeanum* and correlation between their structure and antioxidant activity, PLoS One 9 (2014) 105725.
[11] M.A. Aderogba, A.R. Ndhlala, K.R. Rengasamy, J. Van Staden, Antimicrobial and selected *in vitro* enzyme inhibitory effects of leaf extracts, flavonols and indole alkaloids isolated from *Croton menyharthii*, Molecules 18 (2013) 12633–12644.
[12] H.M. Cho, T.K.Q. Ha, L.H. Dang, H.T.T. Pham, V.O. Tran, J. Huh, J.P. An, W.K. Oh, Prenylated phenolic compounds from the leaves of *Sabia limoniacea* and their antiviral activities against porcine epidemic diarrhea virus, J. Nat. Prod. 82 (2019) 702–713.
[13] F. Gao, D. Zhao, J. Deng, New flavonoids from *Lysimachia christinae* Hance, Helv. Chim. Acta. 96 (2013) 985–989.
[14] K. Slowing, M. Sollhuber, E. Carretero, A. Villar, Flavonoid glycosides from *Eugenia jambos*, Phytochemistry 37 (1994) 255–258.
[15] L.Y. Foo, R. Newman, G. Waghorn, W.C. McNabb, M.J. Ulyatt, Proanthocyanidins from *Lotus corniculatus*, Phytochemistry 41 (1996) 617–624.
[16] K. Ishimaru, G.I. Nonaka, I. Nishioka, Flavan-3-ol and procyanidin glycosides from *Quercus miyagii*, Phytochemistry 26 (1987) 1167–1170.
[17] A. Dübeler, G. Voltmer, V. Gora, J. Lunderstädt, A. Zeeck, Phenols from *Fagus sylvatica* and their role in defence against *Cryptococcus fagisuga*, Phytochemistry 45 (1997) 51–57.
[18] L.J. Porter, Z. Ma, B.G. Chan, Cacao procyanidins: major flavanoids and identification of some minor metabolites, Phytochemistry 30 (1991) 1657–1663.
[19] J.S. Rathore, S.K. Garg, S.R. Gupta, A chalcone and flavanones from *Didymocarpus pedicellata*, Phytochemistry 20 (1981) 1755–1756.
[20] F.M.M. Darwish, M.G. Reinecke, Ecdysteroids and other constituents from *Sida spinosa* L, Phytochemistry 62 (2003) 1179–1184.
[21] A.P. Danelutte, M.B. Costantin, G.E. Delgado, R. Braz-Filho, M.J. Kato, Divergence of secondary metabolism in cell suspension cultures and differentiated plants of *Piper cernuum* and *P. crassinervium*, J. Braz. Chem. Soc. 16 (2005) 1425–1430.
[22] C.F. Lin, T.L. Hwang, C.C. Chien, H.Y. Tu, H.L. Lay, A new hydroxychavicol dimer from the roots of *Piper betle*, Molecules 18 (2013) 2563–2570.
[23] H.A. Priestap, ^{13}C NMR spectroscopy of aristolochic acids and aristololactams, Magn. Reson. Chem. 27 (1989) 460–469.
[24] H. Achenbach, D. Frey, R. Waibel, 6a,7-dehydro-2-hydroxy-4,5-dioxonoraporphine and other alkaloids from *Monocyclanthus vignei*: ^{13}C-NMR studies on 4,5-dioxoaporphines, J. Nat. Prod. 54 (1991) 1331–1336.
[25] K.E. Heim, A.R. Tagliaferro, D.J. Bobilja, Flavonoid antioxidants: chemistry, metabolism and structure-activity relationships, J. Nutr. Biochem. 13 (2002) 572–584.
[26] N. Sato, D. Takahashi, R. Tsuchiya, T. Mukoyama, S.I. Yamagata, N. Satoh, S. Ueda, S.M. Chen, M. Ogawa, M. Yoshida, S. Kondo, Acute nephrotoxicity of aristolochic acids in mice, J. Pharm. Pharmacol. 56 (2004) 221–229.